A Parameterization of the Microphysical Processes Forming Many Types of Winter Precipitation

JULIE M. THÉRIAULT* AND RONALD E. STEWART+

McGill University, Montreal, Quebec, Canada

(Manuscript received 9 June 2009, in final form 14 December 2009)

ABSTRACT

Several types of precipitation, such as freezing rain, ice pellets, and wet snow, are commonly observed during winter storms. The objective of this study is to better understand the formation of these winter precipitation types. To address this issue, detailed melting and refreezing of precipitation was added onto an existing bulk microphysics scheme. These modifications allow the formation of mixed-phase particles and these particles in turn lead to, or affect, the formation of many of the other types of precipitation. The precipitation type characteristics, such as the mass content, liquid fraction, and threshold diameters formed during a storm over St John's, Newfoundland, Canada, are studied and compared with observations. Many of these features were reproduced by the model. Sensitivity experiments with the model were carried out to examine the dependence of precipitation characteristics in this event on thresholds of particle evolution in the new parameterization.

1. Introduction

Various precipitation types often occur during winter storms. These precipitation types include ice pellets and freezing rain as well as particles composed of both liquid and solid phases (Table 1). Precipitation types containing liquid water (such as freezing rain and wet snow) can lead to catastrophic icing events when falling on subfreezing surfaces. One such example is the 1998 ice storm in the Montreal area and surrounding regions, the most catastrophic weather event in Canadian history (Henson et al. 2007).

A particular type of temperature profile, consisting of a warm layer of air (>0°C) aloft and a cold layer below (<0°C), is required to form some of the hazardous types of precipitation (e.g., Wagner 1957; Zerr 1997). These two atmospheric layers are called the melting and the refreezing layer, respectively. Snowflakes falling through a melting layer either melt or partially melt, depending on their size and the atmospheric conditions of the layer. Depending on the degree of melting, these particles may or may not refreeze completely into ice pellets when falling through the refreezing layer before reaching the surface. On the other hand, if the melting layer is just above the surface, fewer precipitation types can form because of the absence of the refreezing layer below.

Several types of precipitation can also coexist because of the particle size distribution. Generally, when falling through a melting layer, smaller particles will be more likely to completely melt whereas larger ones will only partially melt. The collisions between these different types of precipitation can furthermore alter their amounts and sizes or even form another category of particle, as in mixed phase precipitation (Stewart et al. 1990a). For instance, Hogan (1985) states that the freezing of a falling liquid drop can be initiated by a collision with an ice crystal. In this case, it will decrease the amount of supercooled rain and ice crystals and ice pellets are formed. Also, Stewart et al. (1990a) showed that collisions between liquid drops and ice pellets could significantly decrease the amount of freezing rain at the surface.

The microphysical processes associated with precipitation formation and its evolution within numerical

* Current affiliation: National Center for Atmospheric Research, Boulder, Colorado.
+ Current affiliation: Department of Environment and Geography, University of Manitoba, Winnipeg, Manitoba, Canada.

Corresponding author address: Julie M. Thériault, Department of Atmospheric and Oceanic Sciences, McGill University, 805 Sherbrooke West, Montreal, QC H3A 2K6, Canada.
E-mail: julie.theriault@mail.mcgill.ca

DOI: 10.1175/2009JAS3224.1

TABLE 1. Definitions of the hydrometeor categories simulated by the scheme.

Hydrometeor	Symbol	Definition
Rain[a]	r	Precipitation in the form of liquid water drops that have diameters greater than 0.5 mm, or, if widely scattered, the drops may be smaller
Freezing rain[a]	zr	Rain that falls in liquid form but freezes upon impact to form a coating of glaze upon the ground and on exposed objects
Supercooled rain[a]	sr	Liquid precipitation at temperatures below freezing
Snow[a]	s	Precipitation composed of white or translucent ice crystals, chiefly in complex branch hexagonal form and often agglomerated into snowflakes
Ice pellets[a]	ipA and ipB	A type of precipitation consisting of transparent or translucent pellets of ice, 5 mm or less in diameter
Wet snow[a]	ws	Snow that contains a great deal of liquid water
Refrozen wet snow[b]	rws	Refrozen wet snowflake
Slush[b]	sl	Precipitation composed of a mixture of liquid and ice in which the original snowflake's shape is not discernable
Ice crystals[a]	i	Pristine ice crystals
Cloud droplets[c]	c	Small nonsedimenting water droplets
Liquid core pellets[d]	lcp	Partially refrozen drops with an ice shell enclosing liquid water

[a] From Glickman (2000).
[b] From Thériault et al. (2006).
[c] From Milbrandt and Yau (2005b).
[d] From Thériault and Stewart (2007).

models are often simulated using a bulk model approach. A bulk microphysics scheme is based on the assumption that each hydrometeor predicted by the scheme fits an analytic size distribution (e.g., Marshall and Palmer 1948). The bulk microphysics scheme can be a single, double, or triple moment of the analytic size distribution. Many bulk microphysics schemes have been developed to study summer precipitation such as rain and hail (e.g., Kessler 1969; Milbrandt and Yau 2005b). However, less attention has been given to winter storms. In one of the few studies, Szyrmer and Zawadzki (1999) developed a single-moment scheme simulating the melting of snow using an exponential size distribution truncated by the largest snowflakes that have completely melted when falling through the melting layer.

Greater attention is beginning to be paid to the issue of winter precipitation type prediction. For example, as a result of a workshop on winter precipitation issues, Ralph et al. (2005) pointed out that ''the most important problem to be addressed is forecasting winter precipitation types.'' Given the importance of the impact of winter precipitation type formation on the severity of storms and on the ensuing precipitation types, there is certainly a need to develop a more physically based parameterization.

Thériault et al. (2006) began to address the issue of winter precipitation types by developing a double-moment bulk microphysics scheme for several types of precipitation using temperature thresholds. The goal of this study is to go beyond this by improving a bulk microphysics scheme for several types of precipitation using a physically based parameterization. The proposed bulk microphysics scheme builds on the multimoment bulk microphysics scheme developed by Milbrandt and Yau (2005b) and improved to predict winter precipitation types by Thériault et al. (2006). It is used to examine precipitation type formation in a documented event and to conduct sensitivity experiments. It should be noted that it is not the aim of this study to develop a scheme ready to be used in numerical weather prediction models.

This paper consists of several sections. Section 2 is an overview of the microphysics scheme developed in this study. Section 3 is the detailed description of the microphysical sources and sinks. The experimental design is given in section 4. A comparison of the precipitation types produced by the model and observations is discussed in section 5. This includes an examination of the sensitivity of the model results to the parameterizations. Finally, concluding remarks are given in section 6.

2. Overview of the bulk microphysics scheme

The proposed bulk microphysics scheme is built on an existing multimoment microphysics scheme developed by Milbrandt and Yau (2005b). It focuses on the microphysical processes occurring in the lower atmosphere (<4 km). During winter storms associated with a warm front, a melting layer aloft and a refreezing layer below

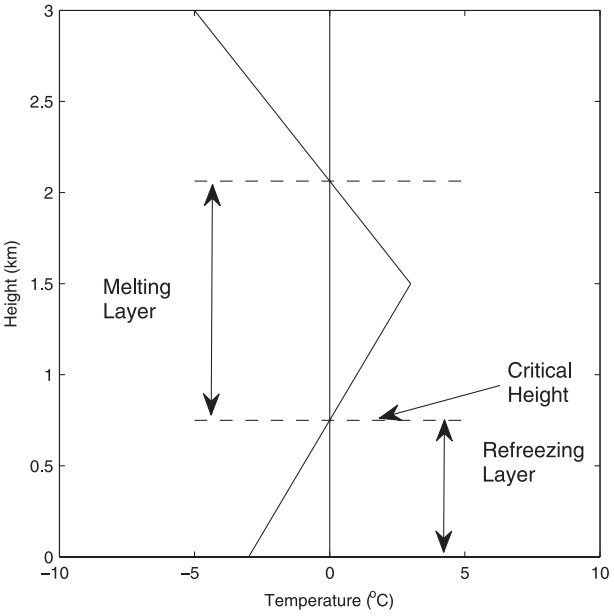

FIG. 1. A schematic of the typical temperature profile often produced during winter storms associated with a warm front. The melting layer aloft refers to a layer with $T > 0$°C and the refreezing layer is the layer with $T < 0$°C below the melting layer. The critical height is the level associated with the bottom of the melting layer and the top of the refreezing layer.

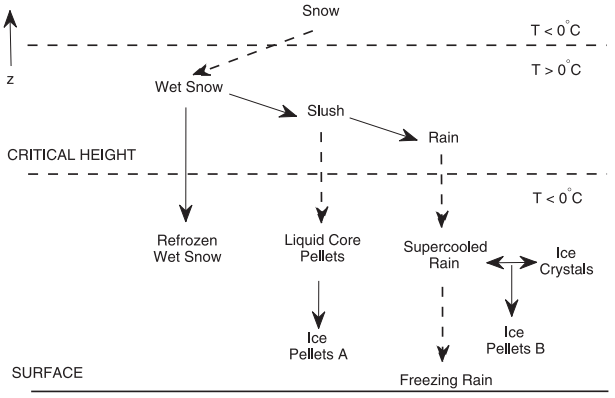

FIG. 2. Schematic diagram of the evolution of precipitation types when falling through the melting layer and the refreezing layer. The critical height is indicated as well as the temperature of the atmospheric layers. The solid line is the ground level. The solid arrows between precipitation-type categories indicate a change of prognostic variables. The dashed arrows indicate that the name of the precipitation changes but they are the same prognostic variables.

are often formed (Fig. 1). Many types of precipitation such as freezing rain and ice pellets may be formed in such atmospheric conditions, compared to only semimelted and liquid particles when the temperature is only decreasing with height. This proposed scheme will be useful in particular for predicting precipitation types associated with temperatures around 0°C. Many microphysics schemes predicting precipitation at temperatures for above or far below this temperature already exist.

a. Precipitation categories

Many precipitation categories have been added to the parameterizations used by Milbrandt and Yau (2005b). The bulk microphysics scheme includes five ice hydrometeor categories [ice crystals (i), snow (s), refrozen wet snow (rws), and two ice pellet categories (ipA and ipB)], two liquid hydrometeor categories [rain (r) and cloud droplets (c)], and one semimelted category [slush (sl)]. In addition, the scheme description also includes more precipitation categories that change depending on whether the temperature is above or below 0°C. For instance, supercooled rain (sr) and liquid core pellets (lcp) are, respectively, rain and slush at temperatures below 0°C and wet snow (ws) is snow when the wet-bulb temperature is above 0°C. Freezing rain will be used to refer to supercooled rain reaching the surface at subfreezing temperatures.

The evolution of the precipitation categories falling through a melting layer and a lower refreezing layer is summarized in Fig. 2. When snow reaches the melting layer it is called wet snow even if it is the same prognostic variable. It is assumed that the smallest snowflakes melt completely before the largest ones. Based on that assumption, wet snow melts partially into slush and slush melts completely into rain when falling through the melting layer.

The type of precipitation reaching the surface largely depends on the liquid fraction of the melting precipitation at the critical height (Fig. 2). For instance, if wet snow reaches the critical height, it will begin to refreeze into refrozen wet snow. On the other hand, if slush reaches the critical height, it is converted into liquid core pellets. Depending on the temperature and depth of the refreezing layer, the liquid core pellets will refreeze partially or completely into ice pellets (ipA) before reaching the surface.

Finally, when falling in the refreezing layer, rain becomes supercooled rain. If ice crystals are locally produced in the refreezing layer, they may interact with supercooled rain to form ice pellets (called ipB). The difference between the two categories of ice pellets is their formation mechanism. One is formed by refreezing semimelted particles (ipA) and the other is formed by contact between supercooled rain and pristine ice crystals or ice nucleation (ipB).

b. Characteristics of the hydrometeor categories

The hydrometeor categories are defined as either a single moment or a double moment of an analytic size

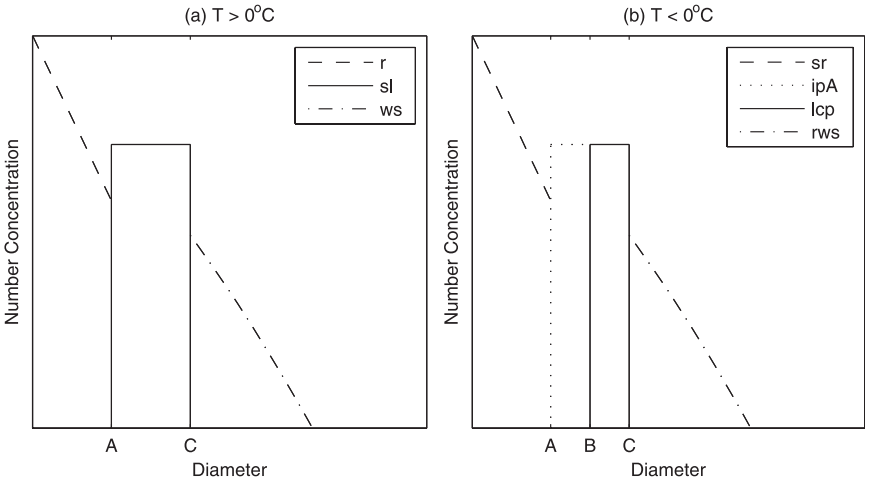

FIG. 3. Schematic diagrams of the size distribution of (a) r, sl, and ws and (b) sr, lcp, and rws; A is the minimum diameter of slush $d_{0\mathrm{sl}}$ and ice pellets $d_{0\mathrm{ip}}$, B is the minimum diameter of liquid core pellets $d_{0\mathrm{lcp}}$ as well as the maximum diameter of ice pellets $d_{0\mathrm{ipA}}$, and C is the maximum diameter of slush $d_{m\mathrm{sl}}$ and liquid core pellets $d_{m\mathrm{lcp}}$.

distribution. A schematic of their size distribution is shown in Fig. 3. The definition of a moment is

$$M_x(n) = \int_0^\infty D_x^n N_x(D_x)\, dD_x, \tag{1}$$

where $M_x(n)$ is the nth moment of the size distribution [(2) and (3)]. Thus, the two moments predicted by the scheme are the zeroth moment ($n = 0$) associated with the total number concentration and the d_xth (Table 2) moment proportional to the mass mixing ratio.

Only the mixing ratio is predicted for slush (liquid core pellets) and ice pellets (ipA) because their sizes are bound by a minimum and a maximum diameter. On the other hand, both the mass mixing ratio and total number concentration are predicted for cloud droplets, rain (supercooled rain), pristine ice crystals, ice pellets B, snow (wet snow), and refrozen wet snow.

All the double-moment categories are described by an analytic size distribution expressed as an exponential function for all the double-moment categories:

$$N_x(D_x) = N_{0x} \exp(-\lambda_x D_x), \tag{2}$$

where $x \in$ c, r(sr), s(ws), rws, ipB. Category r(sr) is truncated by a maximum diameter (d_{mx}), whereas ws and rws are truncated by a minimum diameter (d_{0x}). All the parameters are defined in Tables 3 and 4.

The single-moment categories are characterized by a rectangular distribution bound by a minimum and a maximum threshold diameter. Slush particles are formed under very narrow environmental conditions because they are a mixture of liquid and ice at warm temperatures (Thériault et al. 2006). Since lcp and ipA are formed through the freezing of slush, they are assumed to have the same shape as the slush size distribution. Therefore, the assumed size distribution is

$$N_x(D_x) = N_{0x} \quad \text{for} \quad d_{0x} \le D_x \le d_{mx}, \tag{3}$$

where $x \in$ sl(lcp), ipA. A schematic of their size distributions is illustrated in Fig. 3.

All the hydrometeor categories x have a standard mass–diameter relation. The mass–diameter relation is

$$m_x(D_x) = c_x D_x^{d_x}, \tag{4}$$

where c_x and d_x are defined in Table 2. All the hydrometeor categories are assumed to be spherical with the

TABLE 2. The density and mass–diameter relation for each hydrometeor category. The symbols are defined in Table 1.

Hydrometeor	c_x	d_x	ρ_x (kg m^{-3})	Reference
c	$\frac{\pi}{6}\rho_{\mathrm{c}}$	3	1000	Milbrandt and Yau (2005b)
r(sr)	$\frac{\pi}{6}\rho_{\mathrm{r(sr)}}$	3	1000	Milbrandt and Yau (2005b)
i	$\frac{\pi}{6}\rho_{\mathrm{i}}$	3	500	Milbrandt and Yau (2005b)
s(ws)	0.069	2	—	Field et al. (2005)
rws	0.069	2	—	See text
ipA	$\frac{\pi}{6}\rho_{\mathrm{ipA}}$	3	900	Thériault et al. (2006)
sl(lcp)	$\frac{\pi}{6}\rho_{\mathrm{sl(lcp)}}$	3	1000	Thériault et al. (2006)
ipB	$\frac{\pi}{6}\rho_{\mathrm{ipB}}$	3	900	See text

TABLE 3. List of constants, their units, and description.

Symbol	Value	Units	Definition
a_l	267	$m^{1-b_l}\ s^{-1}$	Terminal velocity parameter of liquid drop (Szyrmer and Zawadzki 1999) used to compute the terminal velocity of wet snow and slush
a_m	82	$m^{1-b_m}\ s^{-1}$	Mean terminal velocity parameter of melting snow
A_F	0.7	—	Constant of the ventilation coefficient for freezing lcp
A_M	1.7	—	Constant of the ventilation coefficient for melting sl and ws
b_l	0.6	—	Terminal velocity parameter of liquid drop (Szyrmer and Zawadzki 1999) used to compute the terminal velocity of wet snow and slush
b_m	0.6	—	Mean terminal velocity parameter of melting snow
B_F	680	$m^{1/(A_F-1)}$	Constant of the ventilation coefficient for freezing lcp
B_M	865	$m^{1/(A_M-1)}$	Constant of the ventilation coefficient for melting sl and ws
C_m	0.87	—	Mean normalized capacitance of melting snowflakes
K_a	*	$J\ m^{-1}\ s^{-1}\ K^{-1}$	Thermal conductivity of air
L_m	334×10^3	$J\ kg^{-1}$	Latent heat of fusion
L_s	283.5×10^4	$J\ kg^{-1}$	Latent heat of sublimation
L_v	250.1×10^4	$J\ kg^{-1}$	Latent heat of evaporation
Ψ	**	$m^2\ s^{-1}$	Diffusivity of water vapor in air

* $0.0078 \times 10^{-2}T + 2.397 \times 10^{-2}$.
** $9.1018 \times 10^{-11}T^2 + 8.8197 \times 10^{-8}T - 1.0654 \times 10^{-5}$.

exception of snow, wet snow, and refrozen wet snow. Their shape is assumed to be an oblate spheroid (Pruppacher and Klett 1997); therefore, their dimension is described by the major axis instead of by diameter as for the spherical particles.

Snowflakes and wet snowflakes have a low density as in Field et al. (2005). The mass–diameter relation and the density of refrozen wet snow are assumed to be the same as for snow and wet snow. A slush particle is mainly composed of liquid water mixed with ice; the snowflake shape has collapsed. Thus, slush is assumed to have the same density as a raindrop because of their similarities.

When slush particles fall in the refreezing layer, they instantaneously start to refreeze into liquid core pellets and it is assumed that they have the same density as slush. Finally, ipA and ipB are assumed to have the density of ice.

Based on the definition of a moment, the total number concentration N_{Tx} and the mass mixing ratio q_{Tx} are defined, respectively, as

$$N_{Tx} = \int_{d_{0x}}^{d_{mx}} N_x(D_x)\, dD_x \quad \text{and} \tag{5}$$

$$q_x = \frac{1}{\rho_{\text{air}}} \int_{d_{0x}}^{d_{mx}} m_x(D_x) N_x(D_x)\, dD_x, \tag{6}$$

where $x \in$ i, r(sr), c, s(ws), rws, ipB, sl(lcp), ip; $N_x(D_x)$ is given by (2) for double-moment categories and by (3) for single-moment categories; c_x and d_x are given in Table 2. The minimum limit of the integral d_{0x} for each category is 0 for r(sr), i, c, s, and ipB, and is >0 for sl(lcp), ipA, ws, and rws. The maximum limit of the integral is truncated for r(sr), sl(lcp), and ipA and tends toward infinity for ws, rws, i, c, s, and ipB. This implies that the total number concentration and the mass mixing ratio are, respectively,

$$N_{Tx} = \frac{N_{0x}}{\lambda_x^{}} \Gamma_{Nx} \quad \text{and} \tag{7}$$

$$q_x = \frac{N_{0x} c_x}{\rho_{\text{air}} \lambda_x^{d_x+1}} \Gamma_{qx}, \tag{8}$$

for $x \in$ i, c, s(ws), rws, ipB; $\Gamma_{Nx} = \Gamma(1, d_{0x}\lambda_x)$ and $\Gamma_{qx} = \Gamma(d_x + 1, d_{0x}\lambda_x)$. For $x \in$ r(sr); $\Gamma_{Nx} = 1 - \Gamma(1, d_{mx}\lambda_x)$ and $\Gamma_{qx} = \Gamma(d_x + 1) - \Gamma(d_x + 1, d_{mx}\lambda_x)$.

Using q_{Tx} and N_{Tx}, the slope parameter λ_x and the intercept of the size distribution N_{0x} are

$$\lambda_x = \left[\frac{N_{Tx} c_x \Gamma(d_x + 1)}{\rho_{\text{air}} q_x}\right]^{1/d_x} \quad \text{and} \tag{9}$$

$$N_{0x} = N_{Tx}\lambda_x, \tag{10}$$

where $x \in$ c, s, ipB, i. For $d_{0x} = 0$, the slope parameter λ_x only depends on q_x and N_{Tx}. On the other hand, for $d_{mx} \neq 0$ or $d_{0x} \neq 0$, the slope parameter λ_x also depends on the threshold diameter. For rain (supercooled rain), the slope parameter is solved using the dichotomy method. For wet snow and refrozen wet snow, a change of variable is applied and the slope parameter depends on the mean mass diameter of the distribution.

TABLE 4. Symbols, values, units, and definition of the parameters.

Symbol	Units	Definition
a_x	$m^{1-b_x}\ s^{-1}$	Terminal velocity parameter of category x
b_x	—	Terminal velocity parameter of category x
c_x	$kg_x\ m^{-d_x}$	Mass–diameter relation parameter of category x
C_x	—	Normalized capacitance of hydrometeor category x
d_{0x}	m	Minimum diameter of category x
d_{fz}	m	Size of a completely frozen liquid core pellet
d_{mx}	m	Maximum diameter of category x
d_x	—	Mass–diameter relation parameter of category x
D	m	Diameter in liquid water equivalent
D_x	m	Diameter of hydrometeor category x. For x = s, ws, rws, it is the dimension of the major axis
E_{xy}	—	Collection efficiency between two hydrometeor categories.
f_x	—	Terminal velocity parameter of category x
$f_{\text{fz}x}$	—	Average liquid fraction of hydrometeor category x at the critical height
f_{lx}	—	Average liquid fraction within hydrometeor distribution x
F_x	—	Ventilation coefficient of category x
$g(f_{lx})$	—	Terminal velocity parameter of melting snow of liquid fraction f_{lx}
k	—	Vertical level
k_{bm}	—	Vertical level at bottom of the melting layer and top of the refreezing layer
k_{top}	—	Vertical level at the top of the melting layer
m_x	kg	Mass of precipitation of hydrometeor category x
$M_x(n)$	—	nth moment of the size distribution of category x
N_{0x}	m^{-4}	Intercept of the size distribution
N_{Tx}	m^{-3}	Total number concentration of category x
$N_x(D_x)$	m^{-4}	Total number concentration per unit volume of particles size D_x
q_x	$kg_x\ kg_{\text{air}}^{-1}$	Mass mixing ratio of category x
t	s	Time since the onset of melting
T	°C	Environmental temperature
T_d	°C	Dewpoint temperature
v_x	$m\ s^{-1}$	Terminal velocity of category x
v_m	$m\ s^{-1}$	Definition of the terminal velocity of melting snow (Szyrmer and Zawadzki 1999)
V_{Nx}	$m\ s^{-1}$	Number weighted-concentration of category x
V_{Qx}	$m\ s^{-1}$	Mass-weighted terminal velocity of category x
x	—	Hydrometeor category described in Table 1
z	m	Height above ground
δq_s	$kg_v\ kg_{\text{air}}^{-1}$	Water vapor mixing ratio difference between the particle surface and the environment
δt	s	Time step of the model
Δd_x	m	Minimum diameter computed during a time step δt
Δd_{70}	m	Particle diameter associated to a liquid fraction of 70% computed during a time step δt
Δt	s	Time of between each vertical level Δz
Δz	m	Vertical grid spacing
γ	—	$\left(\frac{\rho_{\text{sfc}}}{\rho_{\text{air}}}\right)^{1/2}$
$\Gamma(a)$	—	Gamma function: $\int_0^\infty D_x^{a-1} \exp(-\lambda_x D_x)\, dD_x$
$\Gamma(a, b)$	—	Truncated gamma function: $\int_0^\infty D_x^{a-1} \exp(-\lambda_x D_x)\, dD_x$
λ_x	m^{-1}	Slope parameter of hydrometeor category x
ρ_{air}	$kg\ m^3$	Air density
ρ_{sfc}	$kg\ m^3$	Air density at the surface
ρ_x	$kg\ m^3$	Bulk density of category x

TABLE 5. Definition of the terminal velocity–diameter relation for each hydrometeor category. The symbols are defined in Table 1.

Hydrometeor	a_x	b_x	f_x	Reference
r(sr)	4854.0	1.0	195	Milbrandt and Yau (2005b)
i	71.34	0.6635	0	Milbrandt and Yau (2005b)
s	9.7	0.42	0	Milbrandt and Yau (2005b)
ws	11.9	0.42	0	See text
rws	11.9	0.42	0	See text
ipA	206.89	0.6384	0	See text
sl(lcp)	151.36	0.60	0	See text
ipB	206.89	0.6384	0	See text

For the single-moment categories (Table 2), the intercept parameter is derived using the total mass mixing ratio (6) and is expressed as

$$N_{0x} = \frac{q_x \rho_{\text{air}} (d_x + 1)}{c_x (d_{mx}^{d_x+1} - d_{0x}^{d_x+1})} \tag{11}$$

for $x \in$ sl(lcp), ipA.

c. Sedimentation

All the hydrometeor categories are allowed to sediment with the exception of cloud droplets. As in Milbrandt and Yau (2005b), the terminal velocity is described by

$$v_x(D_x) = \gamma a_x D_x^{b_x} \exp(-f_x D_x), \tag{12}$$

where a_x, b_x, and f_x are given in Table 5.

Using the terminal velocity equation for melting snow suggested in Szyrmer and Zawadzki (1999), the wet snow and slush terminal velocity parameters can be derived. The terminal velocity of melting snow as a function of the liquid fraction is

$$v_m(D_r, f_{lx}) \simeq \gamma \frac{a_l}{g(f_{lx})} D_r^{b_l}, \tag{13}$$

where $g(f_{lx}) \simeq 4.6 - 1.8 f_{lx}(1 + f_{lx})$.

According to the melting stages of snowflakes defined by Fujiyoshi (1986), wet snow is defined as stages one to four in which the snowflake shape is still discernable. Slush is associated with stage five in which the shape of the wet snowflake is no longer discernable. A sharp increase of the melting snowflake terminal velocity has been observed at a liquid fraction of approximately 70% by Mitra et al. (1990). Therefore, the threshold liquid fraction between wet snow and slush has been set to 70%. Based on that value, the mean liquid fraction in the wet snow size distribution is 35% and 85% in the slush size distribution. Yuter et al. (2006) show a high variation in the terminal velocity of wet snowflakes of the same sizes. Since there is no obvious pattern, the terminal velocity of wet snow and slush is approximated using (13) for a liquid fraction of 35% and 85%, respectively. For the same reason, the terminal velocity of refrozen wet snow is assumed to be the same as that for wet snow. It is assumed that the shape and the physical size of melting snow only vary when wet snow partially melts into slush. At this point, the snowflake shape is no longer discernable and it looks like a liquid drop.

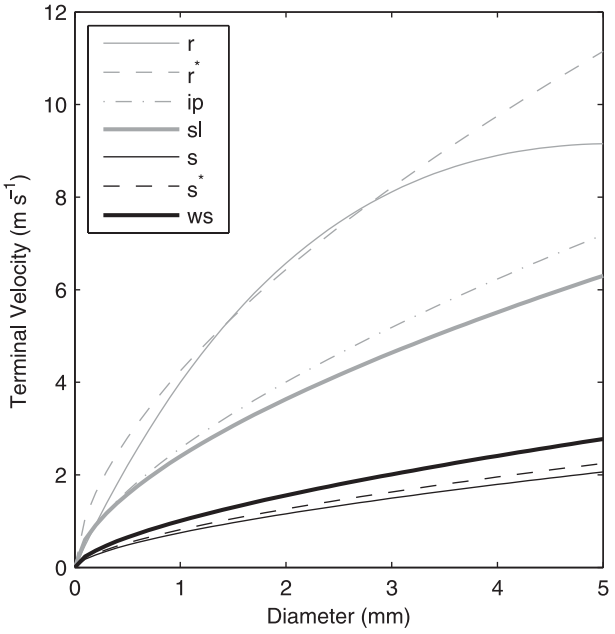

FIG. 4. Comparison of the s, ws, r, sl, and ip terminal velocity used in the scheme (solid line). The symbols *r** and *s** are the terminal velocities used by Szyrmer and Zawadzki (1999) for rain and snow, respectively. The symbols are defined in Table 1.

A comparison of various terminal velocities is shown in Fig. 4. First, the terminal velocities used for snow and rain are comparable to the terminal velocities used in other bulk microphysics schemes such as those of Ferrier (1994) and Milbrandt and Yau (2005b). Second, the slush terminal velocity lies between the rain and wet snow terminal velocities. This is to be expected as slush is composed of both liquid and ice, and it falls faster than wet snow but slower than a completely melted drop for the same liquid water equivalent diameter. Third, since both slush and liquid core pellets are composed of liquid and ice, both precipitation types are assumed to fall at the same terminal velocity. This assumption is supported by the fact that the assumed terminal velocity of slush is comparable the terminal velocity of ice pellets (ipA and ipB).

Sedimentation of the double-moment categories involves both total number concentration and mass mixing ratio (Milbrandt and Yau 2005a,b), whereas only the mass mixing ratio is involved for the single-moment

categories. The mass-weighted q_{Tx} and number-weighted N_{Tx} terminal velocities are given in Milbrandt and Yau (2005a).

3. Microphysics sources and sinks

Several microphysical processes such as melting and freezing of hydrometeors as well as their interactions have been improved in the bulk microphysics scheme developed by Milbrandt and Yau (2005b) to study the formation of winter precipitation types. The following sections describe those improvements. The microphysical sources and sinks affected are listed in the appendix. All the others are described in Milbrandt and Yau (2005b). The symbols for the microphysical sources and sinks are summarized in Fig. 5.

a. Threshold diameters of wet snow and slush

It is assumed that snow is converted into wet snow when the wet-bulb temperature is >0°C; wet snow melts partially into slush and slush melts completely into rain. The rate of the mass of snow melting into liquid water is

$$-\frac{dm_x}{dt} = \frac{2\pi F_x C_x D_x}{L_m}(K_a T - L_v \Psi \rho_{\text{air}} \delta q_s), \quad (14)$$

where $x \in$ ws, sl. According to Szyrmer and Zawadzki (1999), the ventilation coefficient for melting snow is

$$F_x = B_M \frac{D^{A_M}}{D_x}, \quad (15)$$

where $x \in$ ws, sl.

To simulate nonspherical snowflake aggregates, an analogy with electrostatic theory and ice crystal growth is used. A few recent studies such as Westbrook et al. (2008) and Chiruta and Wang (2003) have focused on determining the capacitance of different shapes of snowflakes and aggregates. Because of the high variation of the capacitance depending on the snowflake characteristics, the capacitance of an oblate spheroid with an axis ratio of 0.3 was used (Mitra et al. 1990). Thus, the normalized capacitance used is $C_x = 0.74$ for $x \in$ s(ws), rws. It should be noted that the normalized capacitance is the ratio of the capacitance over the major axis of the particle.

The liquid fraction within a wet snowflake since the onset of melting has been described in Szyrmer and Zawadzki (1999) and is given here as

$$f_{l\text{ws}}(D) = \frac{12 C_{\text{ws}} B_M (K_a T - L_v \Psi \rho_{\text{air}} \delta q_s) t}{L_m \rho_r D^{3-A_M}}. \quad (16)$$

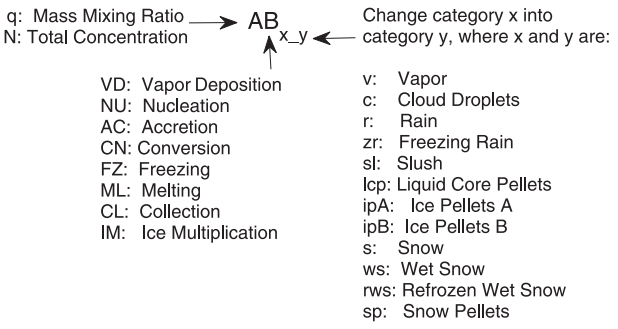

FIG. 5. Definition of the symbols representing the microphysical sources and sinks.

Using (16), the size of the largest snowflake falling from the top of the melting layer k_{top} to vertical level k is

$$d_{0\text{sl}}^{3-A_M} = \sum_{i=k_{\text{top}}}^{k} \left[\frac{12 C_m B_M (K_a T - L_v \Psi \rho_{\text{air}} \Delta q_s)\Delta t}{L_m \rho_r}\right]_i, \quad (17)$$

where k_{top} is the top of the melting layer and k is a level below it. Also, $\Delta t = \Delta z/\gamma a_m D^{b_m}$ where Δz is the vertical grid spacing, $a_m = 82\ \text{m}^{1-bm}\ \text{s}^{-1}$, and $b_m = 0.6$, which corresponds to the terminal velocity of a snowflake that has melted 50% of its mass. Finally, $C_m = 0.87$, which is the normalized capacitance of semimelted snowflakes that have melted up to 50%. This number is calculated by assuming a linear variation of the particle shape with the liquid water fraction.

As in Szyrmer and Zawadzki (1999), the liquid fraction within a given snowflake size is derived using (16) and the generalized relation is expressed as

$$f_l(D) = \left(\frac{D_{\min}}{D}\right)^{1.3}. \quad (18)$$

Thus, the maximum diameter of the slush distribution ($D = d_{m\text{sl}}$) is computed using (18) with $f_{l\text{sl}} = 70\%$ assuming that $D_{\min} = d_{0\text{sl}}$. Since the maximum slush diameter is the threshold diameter between slush and wet snow, the minimum diameter of the wet snowflake size distribution ($d_{0\text{ws}}$) can be computed.

b. Melting of snowflakes

The mass mixing ratio and total number concentration of wet snow melting partially into slush and slush melting completely into rain is described in this section. For simplicity, the melting of slush into rain is described before the melting of wet snow into slush.

The melting of slush into rain depends on the variation of the minimum diameter during one time step δt for each vertical level. Using the inside of the summation in (17),

the variation of the minimum diameter $\Delta d_{\rm sl}$ is obtained. Hence, the mass mixing ratio of slush converted into rain is

$$\Delta q_{\rm sl\_r} = \frac{c_{\rm sl} N_{0\rm sl}}{\rho_{\rm air}} \left(\frac{d_{\rm sl\_r}^{d_{\rm sl}+1} - d_{0\rm sl}^{d_{\rm sl}+1}}{d_{\rm sl}+1} \right), \tag{19}$$

where $d_{\rm sl\_r} = (d_{0\rm sl}^{3-A_M} + \Delta d_{\rm sl}^{3-A_M})^{1/(3-A_M)}$. Similarly, the change in the total number concentration is

$$\Delta N_{\rm sl\_r} = N_{0\rm sl}(d_{\rm sl\_r} - d_{0\rm sl}). \tag{20}$$

The same concept is applied for the melting of wet snow into slush. The largest wet snowflake melting partially into slush during a time step δt is computed using (16) for a liquid fraction of 70% (Δd_{70}). Then, (17) is added to Δd_{70} and converted into real physical snowflake size using the mass–diameter relation (Table 2). Hence, the mass mixing ratio of wet snow changing into slush is

$$\Delta q_{\rm ws\_sl} = \frac{c_{\rm ws} N_{0\rm ws}}{\rho_{\rm air} \lambda_{\rm ws}^{d_{\rm ws}+1}} [\Gamma(d_{0\rm ws}+1, \lambda_{\rm ws} d_{0\rm ws}) - \Gamma(d_{\rm ws\_sl}+1, \lambda_{\rm ws} d_{\rm ws\_sl})] \tag{21}$$

and the total number concentration of wet snow melting partially into slush is

$$\Delta N_{\rm ws\_sl} = \frac{N_{0\rm ws}}{\lambda_{\rm ws}} [\Gamma(1, \lambda_{\rm ws} d_{0\rm ws}) - \Gamma(1, \lambda_{\rm ws} d_{\rm ws\_sl})], \tag{22}$$

where $d_{\rm ws\_sl} = c_{\rm sl}/c_{\rm ws}(d_{m\rm sl}^{3-A_M} + \Delta d_{70}^{3-A_M})^{d_{\rm sl}/[d_{\rm ws}(3-A_x)]}$.

The average liquid fraction within the wet snow distribution is defined as in Szyrmer and Zawadzki (1999) and expressed as

$$f_{l\rm ws} = 0.70(d_{0\rm ws}\lambda_{\rm ws})^{1.3} \frac{\Gamma(1.7, d_{0\rm ws}\lambda_{\rm ws})}{\Gamma(d_{\rm ws}+1, d_{0\rm ws}\lambda_{\rm ws})}. \tag{23}$$

On the other hand, the slush liquid fraction depends only on the minimum and maximum threshold diameters, $d_{0\rm sl}$ and $d_{m\rm sl}$. It is computed using (18) with $D_{\rm min} = d_{0\rm sl}$ and $D = \frac{1}{2}(d_{0\rm sl} + d_{m\rm sl})$.

c. Freezing of slush

When slush reaches the top of the refreezing layer, it starts to refreeze into liquid core pellets. Since slush is composed of a mixture of ice and liquid water, when it reaches subfreezing temperatures, the remaining ice within the particles initiates the freezing. Then, the particle freezes inwards until it is completely frozen into an ice pellet. The inward freezing of drops was first proposed by Johnson and Hallett (1968). This phenomenon has also been inferred by Gibson and Stewart (2007) during an ice pellet storm. A large fraction of observed ice pellets were bulging particles that formed because of rising internal pressure associated with freezing inside an ice shell.

Based on the time to completely refreeze a drop derived in Pruppacher and Klett (1997), the largest liquid core pellets $d_{\rm fz}$ that will completely refreeze at a given vertical level k is

$$d_{\rm fz}^{2-A_F+b_{\rm lcp}} = \sum_{i=k_{\rm bm}}^{k} \left[\frac{12B_F(-K_a T + L_s \Psi \rho_{\rm air} \delta q_s)}{L_m f_{\rm fzsl} \rho_r} \frac{\Delta z}{\gamma a_{\rm lcp}} \right]_i, \tag{24}$$

where $k_{\rm bm}$ is the top of the freezing layer and the ventilation coefficient as a function of diameter can be approximated as $F_{\rm lcp} = B_F D_{\rm lcp}^{A_F}$, where B_F and A_F are constants derived to fit the ventilation coefficient given in Pruppacher and Klett (1997).

The minimum diameter of a completely frozen liquid core pellet $d_{\rm fz}$ is computed as these particles fall through the refreezing layer (24). When that minimum diameter is equal to the minimum diameter of the liquid core pellet distribution ($d_{0\rm fz} = d_{0\rm lcp}$), they start to convert into ice pellets.

The mass mixing ratio of liquid core pellets freezing into ice pellets is based on the minimum diameter variation during one time step δt, and it is expressed as

$$\Delta d_{\rm ip}^{2-A_F} = \frac{12B_F(-K_a T + L_s \Psi \rho_{\rm air} \delta q_s)}{L_m f_{\rm fzsl} \rho_r} \delta t. \tag{25}$$

Hence, the mass mixing ratio of liquid core pellets changed into ice pellets is

$$\Delta q_{\rm lcp\_ip} = \frac{c_{\rm lcp}}{\rho_{\rm air}} N_{0\rm lcp} \frac{d_{\rm lcp\_ip}^4 - d_{0\rm lcp}^4}{4}, \tag{26}$$

where $d_{\rm lcp\_ip} = (d_{0\rm lcp}^{3-A_{\rm lcp}} + \Delta d_{\rm ip}^{3-A_{\rm lcp}})^{1/(3-A_{\rm lcp})}$. When liquid core pellets start to freeze completely into ice pellets, the threshold diameter separating both distributions is $d_{\rm fz}$ (24) and the minimum diameter of ice pellets is the minimum diameter of liquid core pellets at the critical height (top of the refreezing layer). A schematic of the size distribution of ice pellets and liquid core pellets is given in Fig. 3b.

The ice fraction of the liquid core pellet distribution can be computed with (18) by replacing $D_{\rm min}$ with the diameter of the largest completely frozen liquid core pellets (14) and D with the mean diameter of the liquid core pellet distribution $D = \frac{1}{2}(d_{0\rm sl} + d_{m\rm sl})$. The ice

fraction is not allowed to be smaller than the initial ice fraction remaining in the slush distribution at the critical height.

d. Freezing of wet snowflakes

Wet snowflakes are assumed to have liquid droplets formed on the lattice structure of the particles. When they reach the refreezing layer, they automatically start to freeze into refrozen wet snow. For simplification, the heat transfer through the ice shell in the freezing equation is neglected and the equation is reduced to

$$L_m \frac{dm_x}{dt} f_{\text{fzws}} = 2\pi D_x F_x (-K_a T + L_s \Psi \rho_{\text{air}} \delta q_s), \quad (27)$$

where f_{fzws} is the liquid fraction of the wet snow distribution at the critical height (top of the refreezing layer).

The freezing equation is applied to the size distribution of wet snow truncated by its minimum diameter at the critical height. Thus, the mass mixing ratio of wet snow freezing into refrozen wet snow is

$$\text{QFZ}_{\text{ws\_rws}} = \frac{2\pi C_{\text{ws}} B_M N_{0\text{ws}}}{L_m \rho_{\text{air}}} \left(\frac{c_{\text{ws}}}{c_{\text{r}}}\right)^{A_M/d_{\text{r}}} \times (K_a T + L_s \Psi \rho_{\text{air}} \delta q_s) \frac{\Gamma\left(\frac{A_M d_{\text{ws}}}{d_{\text{r}}}, d_{0\text{ws}} \lambda_{\text{ws}}\right)}{\lambda_{\text{ws}}^{A_M d_{\text{ws}}/d_{\text{r}}}}. \quad (28)$$

For simplicity, the variation of the total number concentration ($\text{NFZ}_{\text{ws\_rws}}$) is computed using (28); this follows the approach described in Milbrandt and Yau (2005b).

e. Formation of ice pellets by nucleation

Ice pellets are mainly formed through the refreezing of semimelted particles (ipA). However, depending on the temperature and relative humidity of the refreezing layer, they can be formed through other microphysical processes. These ice pellets are classified as another prognostic variable in the bulk microphysics (ipB).

This process occurs in the refreezing layer near the surface when ice crystals can be formed by deposition nucleation (QNU_{v_i}, NNU_{v_i}) at temperatures < -5°C (Meyers et al. 1992). The ice crystals are collected by supercooled rain and this triggers instantaneous freezing into ice pellets (ipB) ($\text{QCL}_{\text{sr\_i}}$, $\text{QCL}_{\text{i\_sr}}$, $\text{NCL}_{\text{i\_sr}}$). Furthermore, the mass mixing ratio of ipB is enhanced by colliding with supercooled rain. This mechanism increases the mass mixing ratio of ice pellets but not the total number concentration. It also decreases both the mass mixing ratio and total number concentration of supercooled rain ($\text{QCL}_{\text{sr\_ipB}}$, $\text{NCL}_{\text{sr\_ipB}}$).

f. Interactions among hydrometeors

Interactions between particles such as aggregation and collection by other types of precipitation can have a significant impact on the formation of many types of winter precipitation. For example, the melting rate of snowflakes is increased when they fall and collide with cloud droplets and raindrops. These processes are described in Rutledge and Hobbs (1983) and in Milbrandt and Yau (2005b).

The general form of the collection equation for particles of category x collecting particles of category y as well as the bulk collection efficiencies follows the form proposed by Milbrandt and Yau (2005b). The collection efficiencies E_{xy} involving mixed-phase precipitation categories are assumed to be unity. Also, the interactions among ice particles are considered to be negligible. However, snowflake aggregation above the melting layer is allowed ($\text{NCL}_{\text{s\_s}}$). All the liquid categories may interact with solid and mixed-phase categories. The interactions for each category are summarized in the appendix.

g. Sublimation, deposition, and evaporation

In a subsaturated environment with respect to ice, all the solid hydrometeors are allowed to sublimate at any temperature, whereas in a supersaturated environment they can grow by deposition. These processes follow the approach described in Milbrandt and Yau (2005b).

Wet snowflakes are allowed to sublimate and slush is allowed to evaporate. For wet snow, it is assumed that the liquid droplets formed by melting of the lattice structure move inward, allowing ice to directly interact with the environment. Slush, since it is mainly composed of liquid water, is allowed to evaporate (Thériault et al. 2006).

4. Experimental design

The precipitation type characteristics and sensitivity tests have been investigated using the multimoment bulk microphysics scheme (section 3) coupled with a one-dimensional kinematic cloud model. The one-dimensional cloud model has been previously used in studies conducted by Milbrandt and Yau (2005a), Thériault et al. (2006), and Thériault and Stewart (2007). The model is initialized with vertical profiles of temperature T and dewpoint temperature T_d. There are 100 vertical levels evenly spaced with respect to height z over an air column 3 km deep, and hydrostatic balance is assumed.

The cloud model solves the balance equation for both the mass mixing ratio and total number concentration for the double-moment hydrometeor categories and only the mass mixing ratio for the single-moment hydrometeor categories. It should be noted that no horizontal and vertical winds are considered for this study, which only

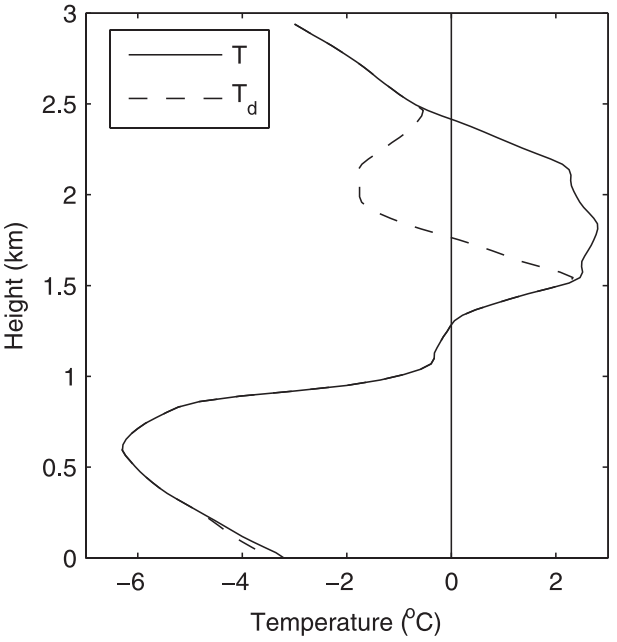

FIG. 6. The temperature T and dewpoint temperature T_d vertical profiles during an ice pellet storm over St. John's, Newfoundland, at 2317 UTC 1 Feb 1992.

considers the effects of temperature and relative humidity on precipitation type formation.

The temperature and moisture profiles (Fig. 6) used to initialize the model were mainly associated with ice pellets at the surface. The observations were taken at St John's, Newfoundland, on 1 February 1992 in an event studied in detail in Hanesiak and Stewart (1995). In the refreezing layer, the environmental conditions were near saturation with respect to water, meaning that it was supersaturated with respect to ice. However, there was a layer of subsaturated conditions at the top of the melting layer. The surface precipitation observed when the sounding was launched (2317 UTC) was ice pellets and needles. Freezing rain mixed with ice pellets and needles was observed at 2345 UTC.

The model was run without changing the environmental temperature and relative humidity. For example, snowflakes are allowed to sublimate into vapor, decreasing the amount of snow but not changing the mass of water vapor. Also, it is assumed that snowflakes continuously fall from the top of the column at a precipitation rate of 2.5 mm h^{-1} to reproduce the surface precipitation rate observed during the storm ($\sim$1 mm h^{-1}). The mass mixing ratio of snow is initialized assuming an N_0 varying with the temperature as in Cox (1988) and falls continuously from above the melting layer. The model is run until a steady state is reached and many features of the bulk microphysics scheme developed can be studied, including the vertical evolution of liquid fraction, precipitation size distribution, and surface precipitation types as compared with observations.

TABLE 6. Summary of the liquid fraction f_{lx} of sl and ws distributions for the four different cases. The terminal velocity v_{Tx} of sl and ws for a 1-mm liquid water equivalent diameter particle based on (13) and varying liquid fraction values.

	f_{lx}		$v_{Tx}(D, f_{lx})$	
Case	ws	sl	ws	sl
A	35	85	1.1	2.4
B	0	70	0.9	1.7
C	70	100	1.7	4.2
D	0	100	0.9	4.2

Sensitivity experiments related to the threshold liquid fraction between wet snow and slush and to their terminal velocities have been carried out using the same temperature and moisture vertical profiles. First, five threshold liquid fractions (50%, 60%, 70%, 80%, and 90%) have been studied. Second, four different scenarios of wet snow and slush terminal velocities have been tested. They are summarized in Table 6. The terminal velocity is related to the liquid fraction of the hydrometeor according to (13). Since the threshold liquid fraction between slush and wet snow is 70%, the wet snow liquid fraction can vary from 0% to 70% and the slush liquid fraction can vary from 70% to 100%. Examples of the terminal velocity varying with the liquid fraction are also given in Table 6. These examples assume a particle liquid water equivalent diameter of 1 mm. The first case (case A) assumes an average terminal velocity of slush and wet snow using an average liquid fraction as described in section 2c. Case B assumes slow-falling slush and wet snow. Case C assumes fast-falling slush and wet snow. Finally, case D assumes slow-falling wet snow and fast-falling slush.

5. Precipitation type characteristics

a. Precipitation types formed

Figure 7a shows the vertical profile of the mass content of each category of precipitation type. When snow starts to melt, it is converted into wet snow. Wet snowflakes eventually melt into slush particles, and slush eventually melts into rain. Because of the subsaturated layer at the top of the melting layer, wet snow only starts to form at 2.25 km. This height corresponds to a wet-bulb temperature above 0°C. Eventually, all the wet snow is converted into slush and a combination of slush and rain reaches the top of the refreezing layer (critical height).

When slush falls into the refreezing layer, an ice shell forms on the surface of the particle and the particles become liquid core pellets. When falling within the

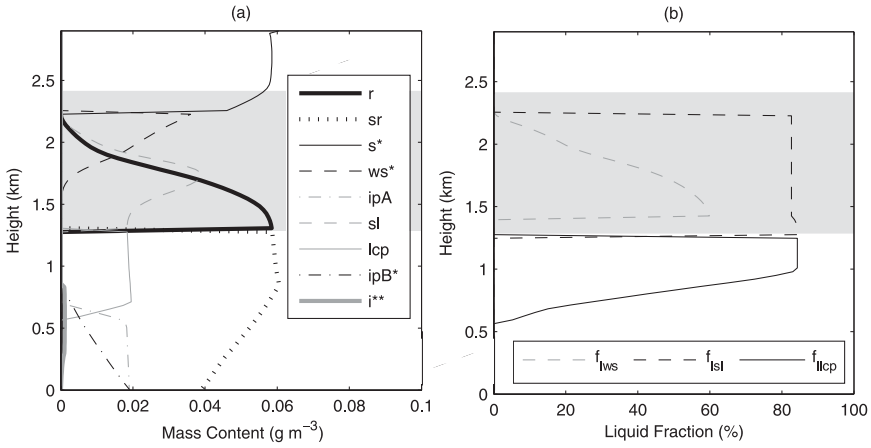

FIG. 7. (a) Vertical mass content profile of the precipitation types formed. The precipitation types marked by one asterisk (*) are scaled by a factor of 0.1 and those marked by two asterisks (**) are scaled by a factor of 100. (b) Liquid fraction of wet snow f_{lws}, slush f_{lsl}, and liquid core pellets f_{llcp}. The gray shading indicates the vertical levels where $T > 0$°C. The symbols are defined in Table 1.

refreezing layer, liquid core pellets freeze gradually until they are completely frozen into ice pellets. The rate of this process depends on the size of the liquid core pellets. Thus, at heights between 500 and 700 m above the ground, liquid core pellets are mixed with ice pellets (Fig. 7a).

Figure 7a also shows that pristine ice crystals are formed within the refreezing layer. These are produced by deposition nucleation. That microphysical process is initiated when the air is supersaturated with respect to ice and when the air temperature is ≤ -5°C. Thus, the ice crystals interact with supercooled rain to form ipB near the surface.

Mainly ice pellets (ipA and ipB) mixed with ice crystals and freezing rain are produced at the surface by the model. This agrees well with the observations reported in Hanesiak and Stewart (1995).

The liquid water fraction within the slush and the wet snow distributions is shown in Fig. 7b. The liquid fraction of wet snow increases with decreasing height within the melting layer. Once it reaches a mean liquid fraction of 60%, the snow has completely melted into slush. At this level, the maximum size of slush remains constant because wet snow has melted completely whereas the minimum diameter of slush keeps increasing with decreasing height because the hydrometeors have not completely melted. Also, the slush liquid fraction is constant because it is assumed to be fixed at 85% until wet snow is completely melted. This is due to the constant liquid fraction within the slush distribution (18). At 1.4 km above the surface, the slush liquid fraction increases when the minimum diameter increases and the maximum diameter remains constant. This occurs when slush is no longer produced because all the wet snow was converted into slush above that level.

Furthermore, there are only small changes in the liquid fraction of liquid core pellets within the top 250 m of the refreezing layer because of the temperature being close to 0°C. The temperature rapidly decreases for the next 500 m and this is correlated with a rapid decrease of the liquid fraction within the size distribution of the liquid core pellets. By a height of 500 m above the ground, all the liquid core pellets have evolved into ice pellets.

The effects of cloud droplets on precipitation type formation were also examined. During warm frontal passages in winter storms that commonly produce the environmental conditions for freezing precipitation, upward motion is generally most prevalent within the melting layer aloft as opposed to the refreezing layer. The cloud droplets produced by this upward motion within the melting layer (<20 cm s^{-1}) did not significantly affect the precipitation types reaching the surface.

b. Precipitation size distribution

The size distributions of all the precipitation types falling through the observed vertical temperature and moisture profiles are shown in Fig. 8. The mean mass diameter of each hydrometeor category is also indicated on each size distribution.

Figure 8a shows the size distribution of wet snow, slush, and rain within the melting layer. The size distribution of raindrops is associated with the smallest particles whereas the wet snow size distribution contains the largest particles because smaller snowflakes melt before larger ones. Furthermore, the slush size distribution is between the rain and wet snow distribution and is bound by a minimum and a maximum diameter (section 3a). The results are also consistent with the assumption that the smallest

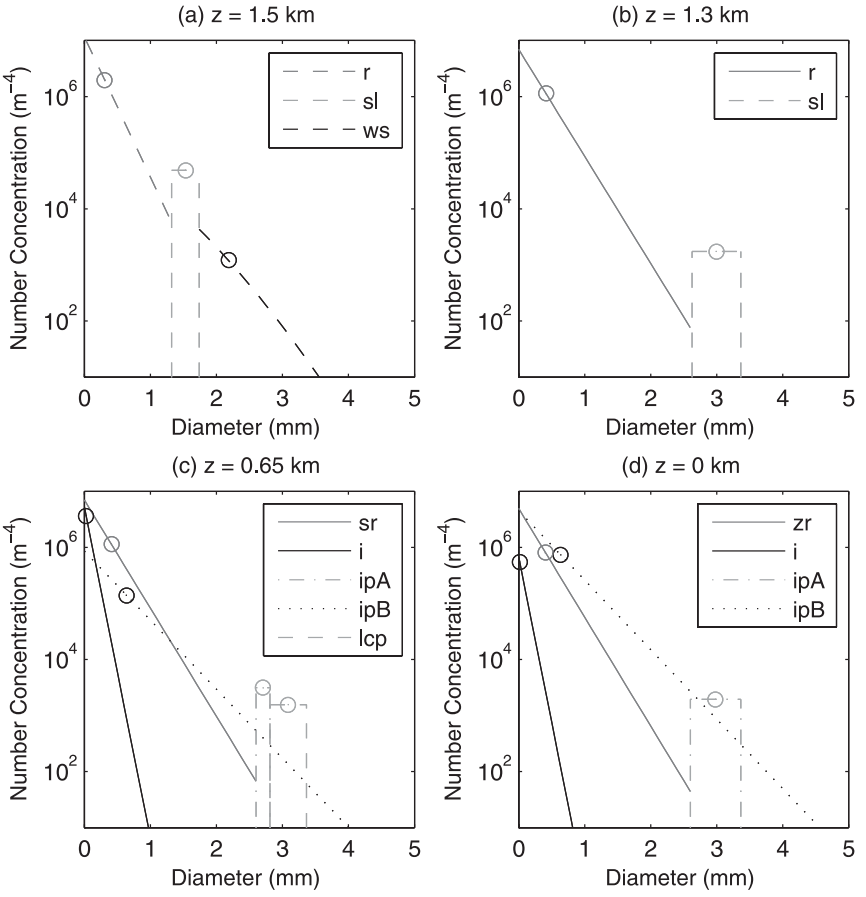

FIG. 8. The size distribution the precipitation types formed at various levels within the melting and refreezing layer: (a) $z = 1.5$ km is within the melting layer, (b) $z = 1.3$ km is at the critical height, (c) $z = 0.65$ km is within the refreezing layer, and (d) $z = 0$ km is at the surface. The symbol ○ shows the mean mass diameter for each hydrometeor distribution. The symbols are defined in Table 1.

particles are completely melted and the largest particles are partially melted snowflakes. The slush size distribution has a mean mass diameter between rain and wet snow.

At the critical height (Fig. 8b), wet snow has completely melted into slush. The mean size of slush at that level is 3 mm and the raindrops have a smaller mean diameter (1 mm).

Figure 8c shows the size distribution of the precipitation types at 650 m. The minimum diameter of ice pellets ($d_{0ip} = 2.7$ mm) and the maximum diameter of liquid core pellets ($d_{mlcp} = 3.3$ mm) are the same as slush at the critical height. The size distribution of three precipitation types—supercooled rain, ice pellets, and liquid core pellets—is consistent with the assumption that the liquid particles are smaller than those produced by partial melting (liquid core pellets and ice pellets). The ice crystals locally produced are the smallest particles. The ice pellets produced by the interaction of ice crystals and supercooled rain (ipB) have mean sizes larger than those of the supercooled drops. Finally, the size of the ipB distribution is smaller than that of the ice pellets formed by the freezing of semimelted particles (ipA).

The size distributions of the precipitation types reaching the surface are shown in Fig. 8d. First, all the liquid core pellets have completely frozen into ice pellets. Second, the size distribution of freezing rain has a shallower slope and a smaller intercept N_0 than at the previous level ($z = 0.65$ km). This is due to the increase in the amount of ipB produced by collisions between locally produced ice crystals and supercooled rain.

6. Sensitivity experiments

Although based on physical insights, several assumptions have been made in the parameterizations of wet snow and slush. To examine the impacts of some of the key aspects, a sensitivity study of the threshold liquid fraction between wet snow and slush and the values of

their terminal velocities has been carried out as described previously in section 4. The sensitivity tests were conducted using the vertical temperature and moisture profiles (Fig. 6) described in section 5.

Figure 9 shows the sensitivity of the surface precipitation types to the threshold liquid fraction. As the threshold liquid fraction increases, the fraction of ipA decreases whereas that of ipB increases. For example, the fraction of ipA is nearly 40% less if the threshold liquid fraction is 90% rather than 50%. In contrast, the fraction of ipB increases with increasing threshold liquid fraction because more mass of slush has completely melted when falling through the melting layer. This increases the mass of supercooled rain in the refreezing layer and leads to more ipB.

Figure 10 shows the sensitivity of surface precipitation types to the terminal velocity of semimelted particles. The terminal velocity is related to the liquid fraction of the hydrometeor according to (13). For example, given the same particle size, the lower the liquid fraction, the slower the particle falls. The different case studies are summarized in Table 6.

These terminal velocity changes lead to significant variations in the surface precipitation types. The fraction of freezing rain decreases with increasing terminal velocity of slush and wet snow and this correlates with an increase of the fraction of ipA. For example, there is nearly 2 times more freezing rain produced in case B than in case C, and case C produces nearly 3 times as many ipA as case B. In contrast, the fraction of ipB only varies by 6% between cases B and C and by nearly 1% between cases A and B. The fraction of ipB decreases since less rain is produced in the melting layer because of the increase in terminal velocity of slush and wet snow and the consequent reduction in the time available for melting.

Figure 10 also shows that the relative fractions of precipitation types produced by cases A and B are comparable but are different from cases C and D. For example, the fraction of ipA reaching the surface is higher assuming fast-falling slush (cases C and D) rather than slow-falling slush (cases A and B) regardless of the wet snow terminal velocity.

Overall, these results suggest that the variation in terminal velocity of slush has a greater impact on the relative amount of precipitation types reaching the surface than the terminal velocity of wet snow, at least for this weather event.

7. Concluding remarks

A physically based parameterization of mixed-phase particles focused on winter storms has been developed.

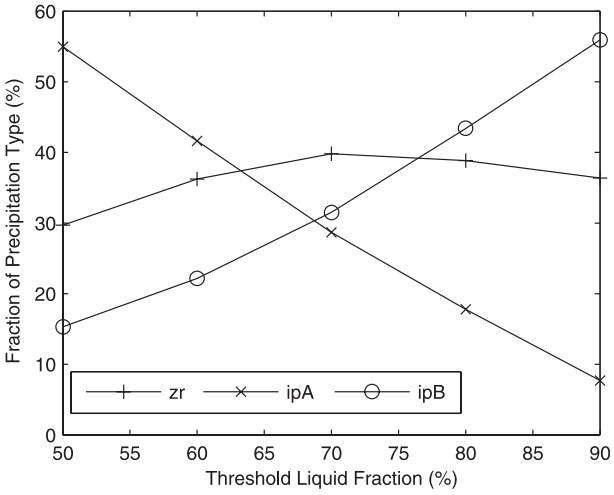

FIG. 9. The influence of the threshold liquid fraction on the surface precipitation types. The surface precipitation types are normalized according to the precipitation rate and the threshold liquid fraction is the liquid fraction differentiating slush from wet snow. The basic parameterization described in section 3 used a threshold liquid fraction of 70%.

It is built on an existing bulk microphysics scheme developed by Milbrandt and Yau (2005b). It accounts for rain (supercooled rain), slush (liquid core pellets), ice pellets, snow (wet snow), refrozen wet snow, and cloud droplets. The concept of truncated size distribution as discussed in Szyrmer and Zawadzki (1999) has been applied to several hydrometeor categories. In addition, the formation of slush, liquid core pellets, wet snow, refrozen wet snow, rain, and supercooled rain is strongly influenced by threshold diameters delineating the stages in the melting process. These were established through physical arguments. The microphysical parameterization also includes the variation of terminal velocity with the degree of melting and freezing as well as the liquid fraction within the mixed-phase categories.

Both single-moment and double-moment hydrometeor categories are defined in the bulk microphysics scheme. The single-moment categories (slush, liquid core pellets, and ice pellets A) have their size distribution bound by a minimum and a maximum diameter. All the other categories are double-moment and their size distributions follow an exponential function. The rain and supercooled rain categories are truncated by a maximum diameter whereas wet snow and refrozen wet snow are truncated by a minimum diameter.

Numerical simulations have been carried out by coupling the bulk microphysics scheme with a one-dimensional kinematic cloud model. In particular, a comparison of the surface precipitation types predicted by the model and

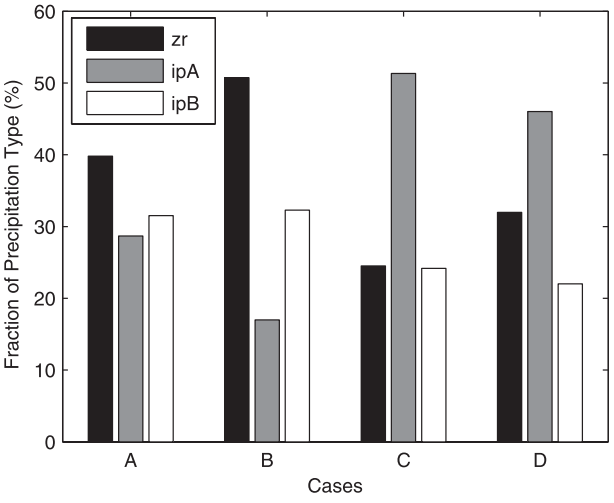

FIG. 10. The surface precipitation types as a function of the terminal velocity of slush and wet snow. The surface precipitation types are normalized according to the precipitation rate. Case A assumes a terminal velocity associated with a mean liquid fraction of slush and wet snow (the basic parameterization described in section 3), case B assumes that slush and wet snowfall at a slower terminal velocity, case C assumes the terminal velocity of the highest threshold liquid of slush and wet snow, and case D assumes wet snow falling as dry snow and slush falling as rain. The basic parameterization is case A. The liquid fraction and terminal velocity for each case are summarized in Table 6.

observed during a storm over St. John's, Newfoundland, on 1 February 1992 (Hanesiak and Stewart 1995) has been carried out. The model produced a mixture of ice pellets, ice crystals, and freezing rain, closely replicating the observations.

Ice pellets were produced by two different mechanisms, which is a new aspect of the bulk microphysics scheme. Most of the ice pellets were formed by the interactions between supercooled drops and ice crystals formed by deposition nucleation near the surface in the simulation. Some ice pellets were also formed by the refreezing of semimelted snowflakes (slush) within the refreezing layer. This illustrates the challenge of accurately simulating the formation of ice pellets during winter storms. Their formation strongly depends on the temperature and depth of the melting layer as well as on the degree of saturation and temperature within the refreezing layer. For instance, if the environmental conditions within the melting layer had been saturated, complete melting of wet snow and slush would have occurred because of the deep (1.5 km) and warm (maximum temperature of 2°C) melting layer. Also, if the refreezing layer had not been supersaturated with respect to ice, no ipB would have formed and more freezing rain would have reached the surface significantly affecting the surface weather conditions.

The size distribution of the precipitation types formed through the observed temperature profile was also examined. Their mean mass diameter is consistent among precipitation type categories. For instance, the sizes of raindrops (supercooled rain) are smaller than those of slush, liquid core pellets, ice pellets, and wet snow. Finally, the mean mass diameter of the ice crystals is very small compared with the other categories of precipitation types. To our knowledge, it is the first time that the size distributions of slush and liquid core pellets have been simulated with numerical models.

The sensitivity of surface precipitation types to the threshold liquid fraction and terminal velocity was investigated. The threshold liquid fraction for slush has an impact on the precipitation types formed at the surface in this particular event. Furthermore, at least in this event, the variation of the slush terminal velocity has a greater impact on the surface precipitation types than that of wet snow. However, in an event with a warmer and deeper melting layer, the threshold liquid fraction and terminal velocity might not have such a strong impact on the surface precipitation types since wet snow and slush would have melted completely.

In summary, a physically based parameterization accounting for many winter precipitation types including wet snow, slush, liquid core pellets, and ice pellets has been developed. This suggested parameterization of precipitation types could be useful when winter storms are associated with precipitation at temperatures near 0°C. This tool can also be used to conduct sensitivity studies of the formation of these precipitation types and their combinations within varying atmospheric forcing.

Acknowledgments. We thank the Natural Sciences and Engineering Research Council of Canada (NSERC) for the financial support needed to accomplish this work. One author (JMT) would like to also thank NSERC, Environment Canada, and McGill University for postgraduate scholarships. The authors would also like to thank the anonymous reviewers for their insightful and helpful comments.

APPENDIX

Microphysics Sources and Sinks

The list of the microphysical sources and sinks of vapor, cloud droplets, and the precipitation categories are given in this section. The symbols are described in Fig. 5. The sources and sinks marked with an asterisk (*) are described or computed as Milbrandt and Yau (2005b).

a. Vapor

$$\left.\frac{\partial q_v}{\partial t}\right|_S = -\mathrm{QVD}_{v\_c} - \mathrm{QVD}_{v\_r} - \mathrm{QVD}_{v\_sr} - \mathrm{QVD}_{v\_sl} - \mathrm{QVD}_{v\_s} - \mathrm{QVD}_{v\_ws} - \mathrm{QVD}_{v\_rws} - \mathrm{QVD}_{v\_ipA} - \mathrm{QVD}_{v\_ipB} - \mathrm{QVD}_{v\_i} - \mathrm{QVD}_{v\_lcp} - \mathrm{QNU}^*_{v\_i}. \quad \text{(A1)}$$

b. Single-moment categories

1) SLUSH (LIQUID CORE PELLETS)

$$\left.\frac{\partial q_{\mathrm{sl(lcp)}}}{\partial t}\right|_S = \mathrm{QVD}_{v\_sl} + \mathrm{QVD}_{v\_lcp} + \mathrm{QML}_{ws\_sl} + \mathrm{QCL}_{r\_sl} + \mathrm{QCL}_{c\_sl} - \mathrm{QML}_{sl\_r} + \mathrm{QCL}_{r\_lcp} + \mathrm{QCL}_{c\_lcp} - \mathrm{QFZ}_{lcp\_ip} - \mathrm{QIM}^*_{lcp\_i}, \quad \text{(A2)}$$

where $\mathrm{QML}_{ws\_sl} = \Delta Q_{ws\_sl}/\delta t$ and $\mathrm{QFZ}_{lcp\_ip} = \Delta Q_{lcp\_ip}/\delta t$.

2) ICE PELLETS A

$$\left.\frac{\partial q_{\mathrm{ipA}}}{\partial t}\right|_S = \mathrm{QVD}_{v\_ipA} + \mathrm{QFZ}_{lcp\_ipA} + \mathrm{QCL}_{sr\_ipA} + \mathrm{QCL}_{c\_ipA} - \mathrm{QIM}^*_{ipA\_i}. \quad \text{(A3)}$$

c. Double-moment categories

1) CLOUD DROPLETS

$$\left.\frac{\partial q_c}{\partial t}\right|_S = \mathrm{QVD}_{v\_c} - \mathrm{QCN}^*_{r\_c} - \mathrm{QAC}^*_{r\_c} - \mathrm{QCL}_{c\_ws} - \mathrm{QCL}_{c\_rws} - \mathrm{QCL}_{c\_lcp} - \mathrm{QCL}_{c\_sl} - \mathrm{QCL}_{c\_s} - \mathrm{QFZ}^*_{c\_i} - \mathrm{QCL}_{c\_ip}, \quad \text{(A4)}$$

$$\left.\frac{\partial N_c}{\partial t}\right|_S = \mathrm{NVD}_{v\_c} - \mathrm{NCL}^*_{c\_c} - \mathrm{NAC}^*_{c\_r} - \mathrm{NCL}_{c\_ws} - \mathrm{NCL}_{c\_rws} - \mathrm{NCL}_{c\_lcp} - \mathrm{NCL}_{c\_ip} - \mathrm{NCL}_{c\_sl} - \mathrm{NCL}_{c\_s} - \mathrm{NFZ}^*_{c\_i}. \quad \text{(A5)}$$

2) RAIN (SUPERCOOLED RAIN)

$$\left.\frac{\partial q_{\mathrm{r(sr)}}}{\partial t}\right|_S = \mathrm{QCN}^*_{r\_c} + \mathrm{QAC}^*_{r\_c} + \mathrm{QVD}_{v\_r} + \mathrm{QML}_{sl\_r} + \mathrm{QML}^*_{i\_r} - \mathrm{QCL}_{r\_sl} - \mathrm{QCL}_{r\_ws} + \mathrm{QVD}_{v\_sr} - \mathrm{QCL}_{sr\_ip} - \mathrm{QCL}_{sr\_lcp} - \mathrm{QCL}_{sr\_rws} - \mathrm{QCL}_{sr\_ipB} - \mathrm{QCL}_{sr\_i} - \mathrm{QCL}_{sr\_ws}, \quad \text{(A6)}$$

where $\mathrm{QML}_{sl\_r} = \Delta Q_{sl\_r}/\delta t$;

$$\left.\frac{\partial N_{Tr(sr)}}{\partial t}\right|_S = \mathrm{NCN}^*_{r\_c} + \mathrm{NAC}^*_{r\_c} - \mathrm{NVD}_{v\_r} + \mathrm{NML}_{sl\_r} + \mathrm{NML}_{i\_r} - \mathrm{NCL}_{r\_sl} - \mathrm{NCL}_{r\_ws} - \mathrm{NVD}_{v\_sr} - \mathrm{NCL}_{sr\_ip} - \mathrm{NCL}_{sr\_lcp} - \mathrm{NCL}_{sr\_rws} - \mathrm{NCL}_{sr\_i} - \mathrm{NCL}_{sr\_ws} - \mathrm{NCL}_{sr\_ipB}, \quad \text{(A7)}$$

where $\mathrm{NML}_{sl\_r} = \Delta N_{sl\_r}/\delta t$.

3) ICE CRYSTALS

$$\left.\frac{\partial q_i}{\partial t}\right|_S = \mathrm{QVD}_{v\_i} + \mathrm{QFZ}^*_{c\_i} - \mathrm{QCL}^*_{i\_s} - \mathrm{QCN}^*_{i\_s} - \mathrm{QML}^*_{i\_r} + \mathrm{QIM}^*_{s\_i} + \mathrm{QIM}^*_{ip\_i} + \mathrm{QIM}^*_{rws\_i} + \mathrm{QIM}^*_{lcp\_i} + \mathrm{QNU}^*_{v\_i} - \mathrm{QCL}_{i\_sr}, \quad \text{(A8)}$$

$$\left.\frac{\partial N_{Ti}}{\partial t}\right|_S = -\mathrm{NVD}_{v\_i} + \mathrm{NFZ}^*_{c\_i} - \mathrm{NCL}^*_{i\_s} - \mathrm{NCN}^*_{i\_s} - \mathrm{NML}^*_{i\_r} + \mathrm{NIM}^*_{s\_i} + \mathrm{NIM}^*_{lcp\_i} + \mathrm{NIM}^*_{i\_i} + \mathrm{NIM}^*_{ip\_i} + \mathrm{NIM}^*_{rws\_i} + \mathrm{NNU}^*_{v\_i} - \mathrm{NCL}_{i\_sr} - \mathrm{NCL}^*_{i\_i}. \quad \text{(A9)}$$

4) SNOW (WET SNOW)

$$\left.\frac{\partial q_{s(ws)}}{\partial t}\right|_S = \mathrm{QVD}_{v\_s} + \mathrm{QCL}^*_{i\_s} + \mathrm{QCN}^*_{i\_s} - \mathrm{QIM}^*_{s\_i} + \mathrm{QCL}_{c\_s} + \mathrm{QVD}_{v\_ws} + \mathrm{QCL}_{c\_ws} + \mathrm{QCL}_{r\_ws} - \mathrm{QML}_{ws\_sl} - \mathrm{QFZ}_{ws\_rws}, \tag{A10}$$

where $\mathrm{QML}_{ws\_sl} = \Delta Q_{ws\_sl}/\delta t$;

$$\left.\frac{\partial N_{Ts(ws)}}{\partial t}\right|_S = -\mathrm{NVD}_{v\_s} + \mathrm{NCN}^*_{i\_s} - \mathrm{NCL}^*_{s\_s} - \mathrm{NVD}_{v\_ws} - \mathrm{NML}_{ws\_sl} - \mathrm{NFZ}_{ws\_rws}, \tag{A11}$$

where $\mathrm{NML}_{ws\_sl} = \Delta N_{ws\_sl}/\delta t$.

5) REFROZEN WET SNOW

$$\left.\frac{\partial q_{rws}}{\partial t}\right|_S = \mathrm{QVD}_{v\_rws} + \mathrm{QFZ}_{ws\_rws} + \mathrm{QCL}_{c\_rws} + \mathrm{QCL}_{sr\_rws} - \mathrm{QIM}^*_{rws\_i}, \tag{A12}$$

$$\left.\frac{\partial N_{Trws}}{\partial t}\right|_S = -\mathrm{NVD}_{v\_rws} + \mathrm{NFZ}_{ws\_rws}. \tag{A13}$$

6) ICE PELLETS B

$$\left.\frac{\partial q_{ipB}}{\partial t}\right|_S = \mathrm{QVD}_{v\_ipB} + \mathrm{QCL}_{sr\_i} + \mathrm{QCL}_{i\_sr} + \mathrm{QCL}_{sr\_ipB}, \tag{A14}$$

$$\left.\frac{\partial N_{TipB}}{\partial t}\right|_S = -\mathrm{NVD}_{v\_ipB} + \mathrm{NCL}_{sr\_i}. \tag{A15}$$

REFERENCES

Chiruta, M., and P. K. Wang, 2003: The capacitance of rosette ice crystals. *J. Atmos. Sci.,* **60,** 836–846.

Cox, G. P., 1988: Modelling precipitation in frontal rainbands. *Quart. J. Roy. Meteor. Soc.,* **114,** 115–127.

Ferrier, B. S., 1994: A double-moment multiple-phase four-class bulk ice scheme. Part I: Description. *J. Atmos. Sci.,* **51,** 249–280.

Field, P. R., R. J. Hogan, P. R. Brown, A. J. Illingworth, T. W. Choularton, and R. J. Cotton, 2005: Parametrization of ice-particle size distributions for mid-latitude stratiform cloud. *Quart. J. Roy. Meteor. Soc.,* **131,** 1997–2017.

Fujiyoshi, Y., 1986: Melting snowflakes. *J. Atmos. Sci.,* **43,** 307–311.

Gibson, S. R., and R. E. Stewart, 2007: Observations of ice pellets during a winter storm. *Atmos. Res.,* **85,** 64–76.

Glickman, T. S., 2000: *Glossary of Meteorology*. 2nd ed. American Meteorology Society, 855 pp.

Hanesiak, J. M., and R. E. Stewart, 1995: The mesoscale and microscale structure of a severe ice pellet storm. *Mon. Wea. Rev.,* **123,** 3144–3162.

Henson, W., R. E. Stewart, and B. Kochtubajda, 2007: On the precipitation and related features of the 1998 ice storm in Montréal area. *Atmos. Res.,* **83,** 36–54.

Hogan, A. W., 1985: Is sleet a contact nucleation phenomenon? *Proc. 42nd Eastern Snow Conf.,* Montreal, QC, Canada, ESC, 292–294.

Johnson, D. A., and J. Hallett, 1968: Freezing and shattering of supercooled water drops. *Quart. J. Roy. Meteor. Soc.,* **94,** 468–482.

Kessler, E., 1969: *On the Distribution and Continuity of Water Substance in Atmospheric Circulations*. *Meteor. Monogr.,* Vol. 32, Amer. Meteor. Soc., 84 pp.

Marshall, J. S., and W. M. Palmer, 1948: The distribution of raindrops with size. *J. Meteor.,* **5,** 165–166.

Meyers, M. P., P. J. DeMott, and W. R. Cotton, 1992: New primary ice-nucleation parameterizations in an explicit cloud model. *J. Appl. Meteor.,* **31,** 708–721.

Milbrandt, J. A., and M. K. Yau, 2005a: A multi-moment bulk microphysics parameterization. Part I: Analysis of the role of the spectral shape parameter. *J. Atmos. Sci.,* **62,** 3051–3064.

——, and ——, 2005b: A multi-moment bulk microphysics parameterization. Part II: A proposed three-moment closure and scheme description. *J. Atmos. Sci.,* **62,** 3065–3081.

Mitra, S. K., O. Vohl, M. Ahr, and H. R. Pruppacher, 1990: A wind tunnel and theoretical study of the melting behavior of atmospheric ice particles. Part IV: Experiment and theory for snow flakes. *J. Atmos. Sci.,* **47,** 584–591.

Pruppacher, H. R., and J. D. Klett, 1997: *Microphysics of Clouds and Precipitation*. 2nd ed. Kluwer Academic, 954 pp.

Ralph, F. M., and Coauthors, 2005: Improving short-term (0–48 h) cool-season quantitative precipitation forecasting: Recommendations from a USWRP workshop. *Bull. Amer. Meteor. Soc.,* **86,** 1619–1632.

Rutledge, S., and P. Hobbs, 1983: The mesoscale and microscale structure and organization of clouds and precipitation in midlatitude cyclones. VIII: A model for the ''seeder-feeder'' process in warm-frontal rainbands. *J. Atmos. Sci.,* **40,** 1185–1206.

Stewart, R. E., R. W. Crawford, N. R. Donaldson, T. B. Low, and B. E. Sheppard, 1990a: Precipitation and environmental conditions during accretion in Canadian east coast winter storms. *J. Appl. Meteor.,* **29,** 525–538.

Szyrmer, W., and I. Zawadzki, 1999: Modeling of the melting layer. Part I: Dynamics and microphysics. *J. Atmos. Sci.,* **56,** 3573–3592.

Thériault, J. M., and R. E. Stewart, 2007: On the effect of vertical air velocity on winter precipitation types. *Nat. Hazards Earth Syst. Sci.,* **7,** 231–242.

——, ——, J. A. Milbrandt, and M. K. Yau, 2006: On the simulation of winter precipitation types. *J. Geophys. Res.,* **111,** D18202, doi:10.1029/2005JD006665.

Wagner, J. A., 1957: Mean temperature from 1000 mb to 500 mb as a predictor of precipitation type. *Bull. Amer. Meteor. Soc.,* **38,** 584–590.

Westbrook, C. D., R. J. Hogan, and A. J. Illingworth, 2008: The capacitance of pristine ice crystals and aggregate snowflakes. *J. Atmos. Sci.,* **65,** 206–219.

Yuter, S. E., D. E. Kingsmill, L. B. Nance, and M. Löffler-Mang, 2006: Observations of precipitation size and fall speed characteristics within coexisting rain and wet snow. *J. Appl. Meteor.,* **45,** 1450–1464.

Zerr, R. J., 1997: Freezing rain: An observational and theoretical study. *J. Appl. Meteor.,* **36,** 1647–1661.